STRENGTH CHARACTERISTICS OF LNG TANKS AND THEIR APPLICATION IN INLAND NAVIGATION

[a]TOMAS KALINA, [b]MARTIN JURKOVIC, [c]MILAN SAPIETA, [d]HELENA BINOVA, [e]ALZBETA SAPIETOVA

[a]University of Zilina, Department of Water Transport, Univerzitna 1, 010 26 Zilina, Slovakia
[b]University of Zilina, Department of Water Transport, Univerzitna 1, 010 26 Zilina, Slovakia
[c]University of Zilina, Department of Applied Mechanics, Univerzitna 1, 010 26 Zilina, Slovakia
[d]CTU Prague, Department of Logistics and Management Transport, Konviktska 20, Prague 110 00, Czech Republic
[e]University of Zilina, Department of Applied Mechanics, Univerzitna 1, 010 26 Zilina, Slovakia

email: [a]tomas.kalina@fpedas.uniza.sk, [b]martin.jurkovic@fpedas.uniza.sk, [c]milan.sapieta@fstroj.uniza.sk, [d]binova@fd.cvut.cz, [e]alzbeta.sapietova@fstroj.uniza.sk

Abstract: EU legislation in the field of transport and energy is focused on the safety of transport and storage of LNG, environmental friendliness, but above all to protect the health of the population. LNG is an important alternative to conventional ship fuel. Under current IMO guidelines and ADN, LNG fuel tanks installed in the vessel must meet the criteria of the LNG tank from a group of "independent types A, B, or C". Specifically, the fuel tanks of inland waterway vessels are the type "C". One method for determining the strength characteristics of the LNG is the tank finite element method (FEM), which is evaluated using the HMH stress hypothesis. The result is a set of the maximum stress characteristics and assessment of the suitability of LNG tanks on inland vessels and floating terminals.

Keywords: LNG, LNG storage, strength characteristics, computation model, stress tests

1 Introduction

Energy security and independence from fossil fuel imports from Russia is one of the most frequent economic - political issues in Central and Eastern Europe. Trade in strategic raw materials is becoming an effective political tool for creating spheres of influence in the regions, and thus a potential source of conflict. One way to prevent this is to diversify sources.

Natural gas is the most used energy source after oil and black coal. It is expected that its consumption will rise in the future. Not only worldwide but also in the European Union. The consumption of the natural gas in the world will drag the emerging economies, mainly Asian countries. In the European Union, it currently leads trend of "green" energy sources and low-carbon fuels.

The most strategic of natural gas is the wide range of applications. In addition to traditional technologies using natural gas as a producer of the electricity and heat nowadays are here new opportunities especially in transport. Increasingly stringent standards aimed at emissions (mainly CO_2, NO_x, SO_x), and particulate matter (PM) from transport are forcing carriers to look for the solutions to eliminate these negative aspects, considering not only environmental but also economic aspects (Tropp et al., 2012). In this regard, some of the most promising solutions offer alternative fuel technology. Compared to conventional fuels, liquefied natural gas (LNG) can reduce NO_x by up to 85-90 %, SO_x and PM by close to 100 % and CO_2 by 15-20 % (GIIGNL).
Road transport companies are faced with this problem for decades. The first European emission standards Euro 1 took into effect in 1993. Compliance with this standard required a substantial change of engine elements such as installation controlled three-way catalytic converter and lambda probe. In comparison with the situation in 1993, currently applicable emission standards Euro 6 have brought the reduction of PM by 99 % and NO_x by 98 % (GIIGNL).

The first European legislative regulation concerning to the emission limits for inland transport appeared in 2004. Directive 2004/26/EC complementing Directive 97/68/EC regulated emissions of new engines installed on inland vessels for the period until the end of 2008. Responding to developments in road transport has brought further adjustments in the adjustment of Directives 2010/26/EU and 2012/46/EU mainly focused on modulating NO_x emissions. The last legislative amendment was approved by the European Parliament in July 2016. Within the "phase V" Directive tightens emission limits for combustion engines of non-road mobile machinery and also inland navigation ships. These measures are accompanied by broader support of the research in the field of alternative fuels. Inland water transport clearly preferred the use of dual fuel systems (diesel – LNG). Wider application of the LNG in transport avoids the need for a functioning market (Barta et al, 2016). This is related to the resolution of the many problems with logistics, not only within the region but also with regard to the production regions and physical properties related to LNG being transported over long distances. It is necessary for solving the many problems with the logistics, not only in the region of the production, but also due to the other participating regions within the logistics chain with respect to the physical properties of LNG related to its transportation over long distances. Currently the legislation applying to the transportation of dangerous goods (ADR) allows using the LNG tankers on the inland waterways. Tankers should be equipped with special containers - tanks for the storage of cryogenic gases Similar tanks are also possible for use for long-term storage in the central terminal. Although this technology is not new, its application to inland vessels has only just begun. During the designation and location of the containers to an existing vessel the shape of the tank and the amount of stored gas, as well as insulation and strength characteristics must be considered (Sebor et al, 2006).

2 The legislative framework and the safety of transportation and storage of LNG

Legislation in the field of transport, storage and distribution of LNG in the world is different. The main idea is to ensure safety in transportation and storage of LNG, environmental friendliness, but especially health protection. Nowadays, in the boom of implementation of LNG as an alternative fuel in the transport and energy sectors in Europe, it is necessary to implement safety risk assessment according to accepted methodologies. European regulations mainly focus on the outcomes regardless of the ways to achieve required level of safety (GIIGNL).

EC (European Council) Directive 2012/18/ EU (SEVESO III) is aimed at preventing accidents and prevention of conflicts of transport of dangerous substances such as the LNG. The directive was drawn up based on Council Directive 82/501/EEC (SEVESO I) and EC Directive 96/82/EC (SEVESO II). On the revision of SEVESO I and SEVESO II it was based on an assessment of major accidents and analysis of the failure of safety management systems for the transportation of LNG (European Commission – SEVESO III).
European Committee for Standardization (CEN) defines codes and regulations relating to import LNG:

- European Union SEVESO III Directive 2012/18/ EU of 1 June 2012;
- EN 1473: „Installation and equipment for LNG – Design of onshore installations ". Designed for storage capacities over 200 tones. This code is based on a risk assessment approach;
- EN 1160: „Installation and equipment for LNG – General characteristics of LNG ";
- EN 14620: „Design and manufacture of site built, vertical, cylindrical, flat-bottomed steel tanks for the storage of

refrigerated, liquefied gases with the operating temperatures between 0°C and – 165°C;

- EN 1474: „Design and testing of LNG loading/unloading arms";
- EN 13645: „Design of onshore installations with a storage capacity between 5 tones and 200 tones "(CEN).

According to ADN (European Agreement Concerning the International Carriage of Dangerous Goods by Inland Waterways) maximum volume of the tank type G1 designed for the transportation of LNG by inland waterways is 380 m^3. Due to the expected size of vessel (in case of pushing convoys is a type DE IIb) is the maximum volume at 350 m^3 (European Commission – SEVESO III).

3 Research questions and the focus of the study

The paper focuses primarily on the assessment of two research questions: (*1) what are complying with the design parameters of LNG tanks for the transport and storage of LNG for inland vessels and inland LNG terminals? (2) What are the basic strength parameters, which must comply with tanks?* Design of suitable reservoirs depends on several factors (purpose, ship size, the parameters of the waterway, LNG terminal capacity etc.). Therefore, is necessary within the solving of the research questions consider mentioned aspects.

4 The basic design parameters of LNG tanks

Due to the physical properties of LNG, its transport and long-term storage must necessarily bring a wide range of mainly safety and technical issues. A significant role plays here also the economical and the environmental aspects. To solving all these aspects have been expended great resources. It brought a wide range of technical solutions in storage technology useful not only in inland terminals but also for vehicles (Skrucany et al, 2015).

For vessels transporting liquefied natural gas, current legislation allows to use 4 types of tanks:

- membranes tanks,
- independent self-supporting tanks:
  - type A,
  - type B,
  - type C.

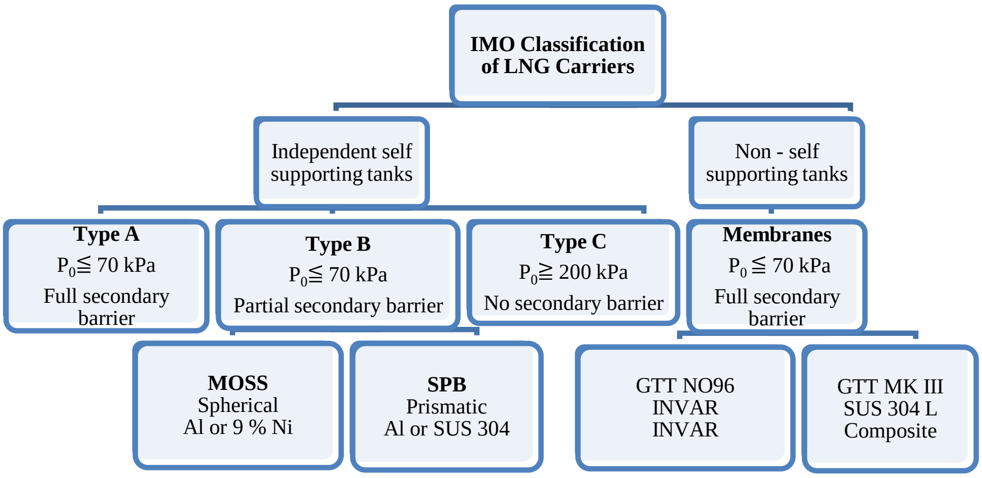

Figure 1 Classification of LNG Carriers according IMO (*Source: GIIGNL)*

LNG fuel tanks must comply the criteria of Independent self-supporting tanks (type A, B, or C) according to the IMO and ADN legislation (Figure 1). Specifically, the fuel tanks of inland vessels must comply with type C.

From a technical and operational point of view using of reservoirs "C" provides several benefits:

- IGC (The International Code for the Construction and Equipment of Ships Carrying Liquefied Gases in Bulk) does not required secondary barrier for this type of tank,
- Small and medium sized tanks can be designed with vacuum insulation, which saves insulating material and it increases the efficiency of the insulation,
- Simple installation (for the storage of the tanks are sufficient two suitable shaped supports,
- Ability to design the tanks for high pressure, which is good for long-term storage and solving problems with evaporation.

From a structural point of view these are mostly double-skin pressure tanks cylindrical shape with an arched bottom. The inner tank is made of austenitic stainless steel or 9% nickel steel. The outer container, which acts as a secondary barrier can be made from either stainless steel or carbon steel. The wall thickness of the inner and outer container is at least 3 mm. The space between them is isolated by a combination of Perl / vacuum or Multi-Layer Insulation (MLI) / vacuum. The tank is equipped with fittings for filling, pressure regulators, taking into LNG heat exchanger, measuring level and pressure (Hoffman, 2016). Standard tanks are designed for the pressure of 1.6 MPa. The real operating pressure depends on the needs of the engine and the injection device fluctuates from 0.3 to 1 MPa (Buil, 2013). LNG technology differs from CNG technology only in tanks and evaporation, other technological elements are in both same. The design must meet the requirements of the IMO IGC "International Code for the Construction and Equipment of Ships designed for liquefied gas" and EN 13458-2 "for cryogenic vessels (IMO).

5 Assessment of strength characteristics of LNG tanks

Solution of strength characteristics of LNG tanks was carried out by finite element method (FEM), which were evaluated using the HMH stress hypothesis, i.e. hypothesis of maximum specific deformation energy required to change shape. This hypothesis gives the most accurate value and is most commonly used. It is used in the computation software where reduced stress by HMH strength hypothesis is called Von Misses stress. It is suitable for ductile materials. The criterion of dangerous condition is maximum specific strain energy required to change shape $\lambda_{t\,max}$. Strength HMH hypothesis assumes that a dangerous condition occurs when the specific strain energy for changing the shape of the stress state exceeds specific strain energy to change the shape of rectilinear con stress state, which results in failure. Requires the fulfilment of inequality:

$$\lambda_{t\,max} \leq \lambda_D, \qquad (1)$$

where:
$\lambda_{t\,max}$ maximum specific strain energy,
λ_D maximum allowable strain energy.

Dangerous condition occurs in the specific strain energy for changing the shape:

$$\lambda_D = \frac{1+\mu}{3E}\sigma_D^2, \quad (2)$$

where:
μ poisson ratio,
E Young's modulus,
σ_D maximum allowed stress.

Whichever is:

$$\lambda_{t\,max} = \frac{1+\mu}{3E}(\sigma_1^2 + \sigma_2^2 + \sigma_3^2 - \sigma_1.\sigma_2 - \sigma_1.\sigma_3 - \sigma_2.\sigma_3), \quad (3)$$

where:
σ_1 first principal stress,
σ_2 second principal stress,
σ_3 third principal stress.

Parameters $\sigma_{1,2,3}$ are principal stresses in each direction. Substituting relations (2) and (3) to (1) and by adjusting receive strength condition according HMH hypothesis for the spatial state of stress:

$$\sigma_{red} = \sqrt{\sigma_1^2 + \sigma_2^2 + \sigma_3^2 - \sigma_1.\sigma_2 - \sigma_1.\sigma_3 - \sigma_2.\sigma_3} \leq \sigma_D, \quad (4)$$

where:
σ_{red} reduced stress according HMH hypothesis.

For planar state of stress is valid relation:

$$\sigma_{red} = \sqrt{\sigma_1^2 + \sigma_2^2 - \sigma_1.\sigma_2} \leq \sigma_D. \quad (5)$$

For planar state of stress given by the normal and shear stresses τ:

$$\sigma_{red} = \sqrt{\sigma^2 + 3\tau^2} \leq \sigma_D, \quad (6)$$

where:
τ shear stress.

Using HMH strength hypothesis, it is possible to calculate the reduced stress without the knowledge of the principal normal stresses. The reduced stress can be directly calculated for a given state of stress by 6 independent components of the stress:

$$\sigma_{red} = \frac{\sqrt{2}}{2}.\sqrt{(\sigma_x - \sigma_y)^2 + (\sigma_y - \sigma_z)^2 + (\sigma_z - \sigma_x)^2 + 6.(\tau_x^2 + \tau_y^2 + \tau_z^2)} \leq \sigma_D, \quad (7)$$

where:
σ_x normal stress in directions X,
σ_y normal stress in directions Y,
σ_z normal stress in directions Z,
τ_{xy} shear stress in directions X,
τ_{yz} shear stress in directions Y,
τ_{xz} shear stress in directions Z.

The maximum allowed stress can be seen from relation:

$$\sigma_D = \frac{Re}{k}, \quad (8)$$

where:
Re yield strength for the material,
k safety factor (for the chosen material mostly determined by relevant standard),
σ_D maximum allowed stress.

In the case of LNG tanks, which are the subject of this paper, safety factor is determined by IMO standard. This standard prescribes a safety factor $k = 1.5$ for all load cases specified in this standard (Lisowski et al, 2010).

Computational models of vessels were made based on ideological proposals, where individual dimensions were chosen. Models were modified so that the all parts that do not affect the stress have been removed from ideological models. For stress analysis, it has not been take into account the strength of insulation. Its impact was specified as the mass on the inner shell (Stopka et al, 2016).

5.1 Loading

Maximum allowed working pressure of tanks is prescribed up to 10 bar it was prescribed on inner shell. Vacuum between shells was prescribed like pressure of the value 130 MPa on the internally sides of shell and atmospheric pressure of value 101,325 kPa prescribed on external side of outer shell. Portable tanks and their fastenings should be capable of withstanding separately applied forces, based on:

1. twice the total mass acting in the direction of travel of the tank simultaneous with the weight of the tank;
2. the total mass acting horizontally at right angles to the direction of travel of the tank (where the direction of travel is not clearly determined, the total mass should be used) simultaneous with the weight of the tank;
3. the total mass acting vertically upwards;
4. twice the total mass acting vertically downwards.

Impact of LNG was included in the computation by the hydrostatic pressure as follows according to standard four load cases (Figure 2).

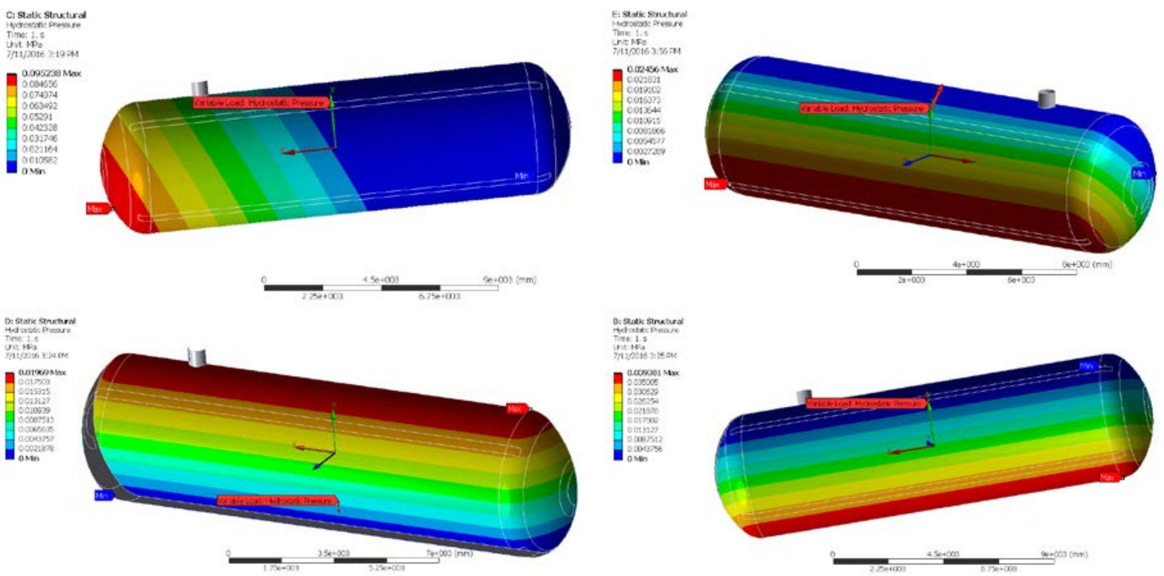

Figure 2 Hydrostatic pressure for all load-cases *(Source: authors)*

5.2 Boundary conditions

All degrees of freedom in model were taken in site of attachment vessels with a ship decks area marked in blue (Figure 3).

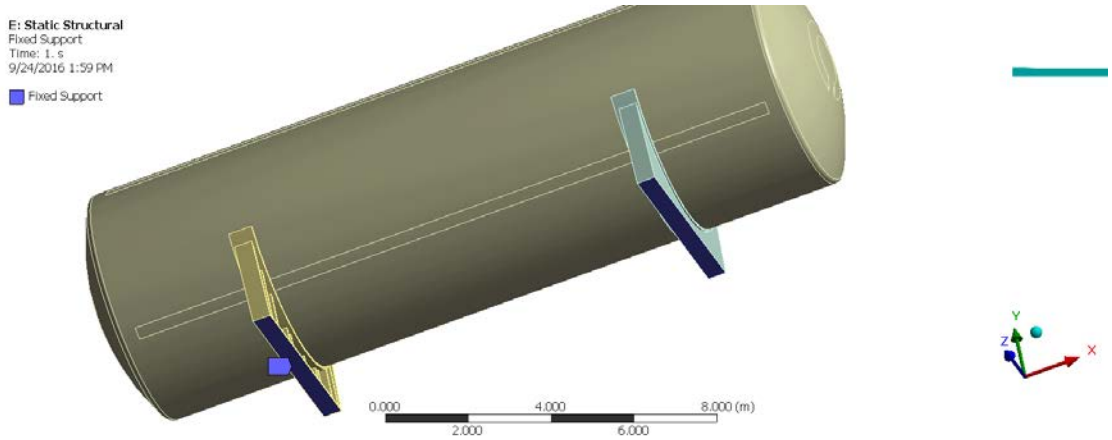

Figure 3 Location of fixed support on model - blue color *(Source: authors)*

5.3 Material properties

As indicated above, the selected material of the outer and the inner shell is stainless steel AISI 304. For longitudinal support and knobs was selected plastic material polycarbonate for the good ratio between strength and insulating properties. The material properties for the assessment of the strength properties are given in Table 1.

Material	Young´s modulus [GPa]	Poisson´s ratio
AISI 304	200	0,29
Polycarbonate	2,21	0,37

Table 1 Material properties *(Source: GIIGNL)*

The material properties are dependent on the operating temperature. As mentioned above, the temperature of LNG is about -160° C and temperature of environment was considered 20° C. The necessary properties such as yield strength and ultimate strength for both materials in given temperatures are indicated in Table 2.

Material	Temperature [°C]	Yield Strength [MPa]	Tensile Strength [MPa]
AISI 304	20°C	205	515
	-160°C	380	1470
Polycarbonate	20°C	70	

Table 2 Tensile properties at varying temperatures *(Source: GIIGNL)*

5.3.1 FEM mesh

Mesh of elements was created on the geometric model for the purpose of calculation, using FEM. The outer and inner shells were meshed by shell-elements for the remaining items in the assembly (plastic supports longitudinal and knobs, stand under the tank) were used volume elements.

For three loading states half symmetry was used. Model consist of 1 939 766 elements. In this case, it was necessary to calculate the whole model, and the number of elements increased to 3 914 394 from which were created 6 363 429 equations in the computational model (Figure 4 and Figure 5).

In Figure 4 and Figure 5 it is possible see the created FEM mesh for LNG tank. Figure 4 shows the outer shell with the supports and Figure 5 shows the inner shell with plastic longitudinal supports and knobs.

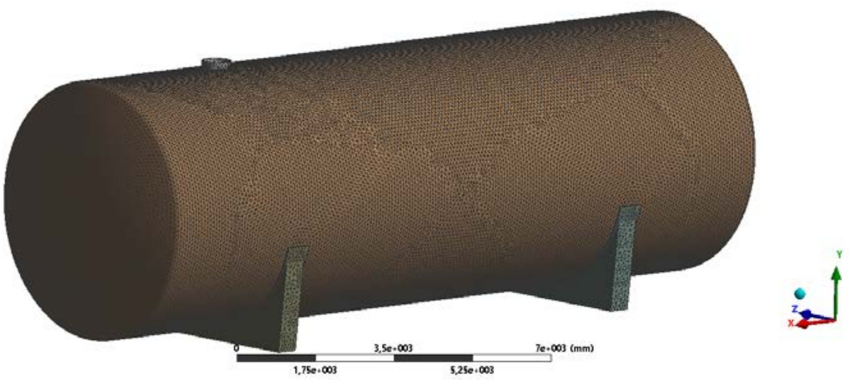

Figure 4 Mesh of outer shell of LNG vessel volume 348,5 m^3 *(Source: authors)*

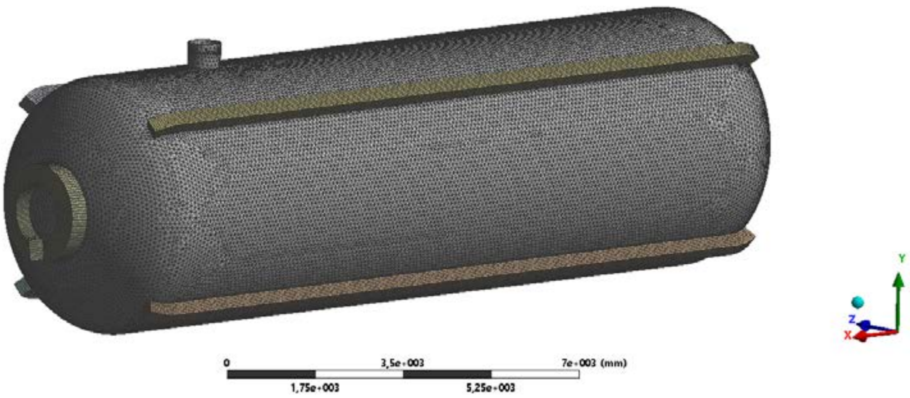

Figure 5 Mesh of inner shell of LNG vessel volume 348,5 m^3 *(Source: authors)*

5.4 Results of computation

As Substituting of all the necessary parameters such as load, boundary conditions and material model, the load cases 1-4 were obtained distribution of stress fields, as shown in Figures 6 – 13. In neither of these cases did not exceed the maximum stress allowable stress which gives the IMO standard.
Each analysis was calculated on the computational server. For the calculation were used processors with attribution Intel Xeon E5-v4640 0 2.4GHz with 32 calculation cores, allocated memory for the first three analysis was till 78 GB and for last analysis was this value about 178 GB. Computation time of the first three analyses was around 90 minutes and for the last analysis, it was 282 minutes.

The results of all load cases are stress distribution plotted in two views namely in the case where the stress distribution is shown in outer shell, and in the case where the stress distribution is shown on the inner shell.

5.4.1 Results for load state 1

The stress distribution at the first load cases can be seen in Figure 6 and Figure 7. The maximum value of stress on outer shell is in front part, the position is marked with a red arrow (Figure 6). In the case of the inner shell, the maximum value of stress is around the filler neck and it is also marked with a red arrow (Figure 7).

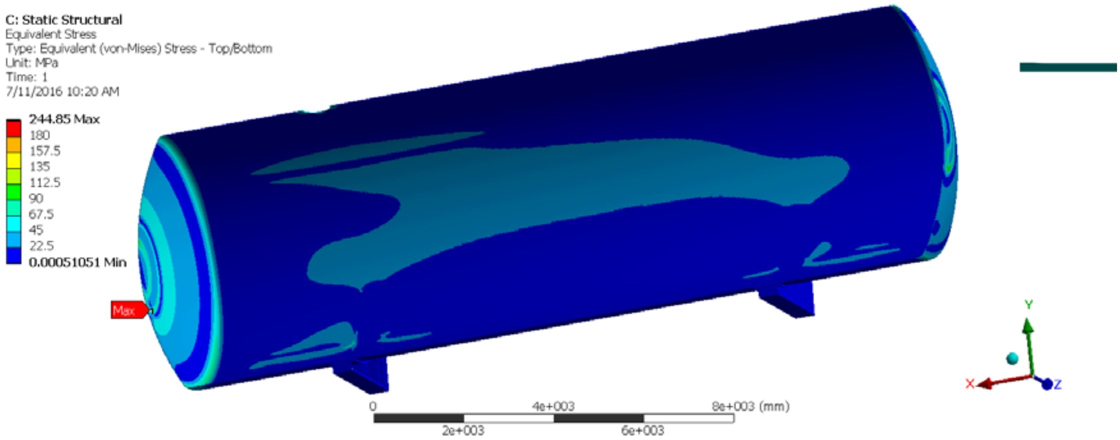

Figure 6 Load case 1 - stress distribution on outler shell *(Source: authors)*

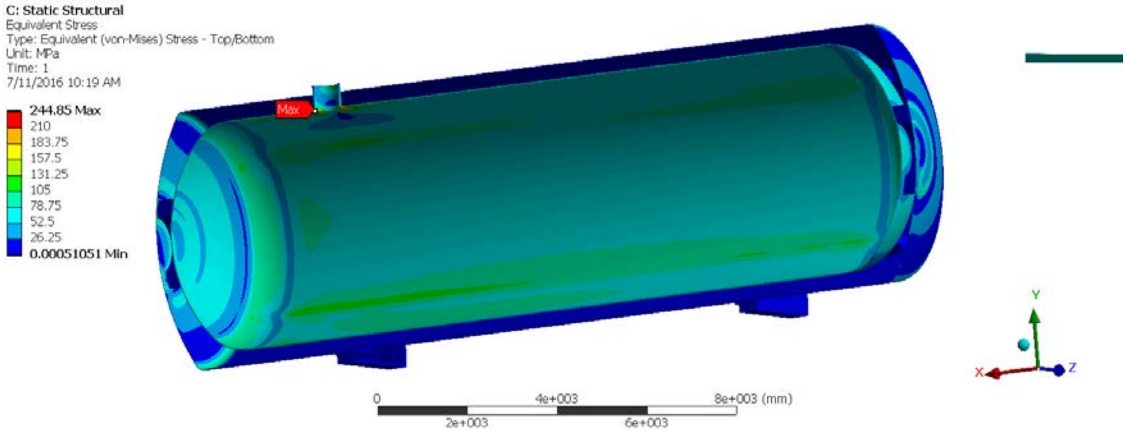

Figure 7 Load case 1 - Longitudinal crossection stress, distribution on inner shell *(Source: authors)*

The maximum values of stress are shown in Table 3, which also contains the value of the calculated safety factor. Safety factor does not fall below the permissible value of 1.5 in either load case, so construction can be considered satisfactory for this load state.

Part	Equivalent von Misses stress [MPa]	Safety factor
Inner shell	244,85	1,55
Outer shell	129,99	1,57

Table 3 Load case 1, comparison of calculated values and allowed values (*Source: authors)*

5.4.2 Results for load state 2

In the second load cases, it was not possible to use half the symmetry due to asymmetrical nature of the load. In computation, the whole model was used. The maximum stress value of the outer shell is in the front part the shell (Figure 8). The maximum value of stress in inner shell was again in the area of the filler neck (Figure 9).

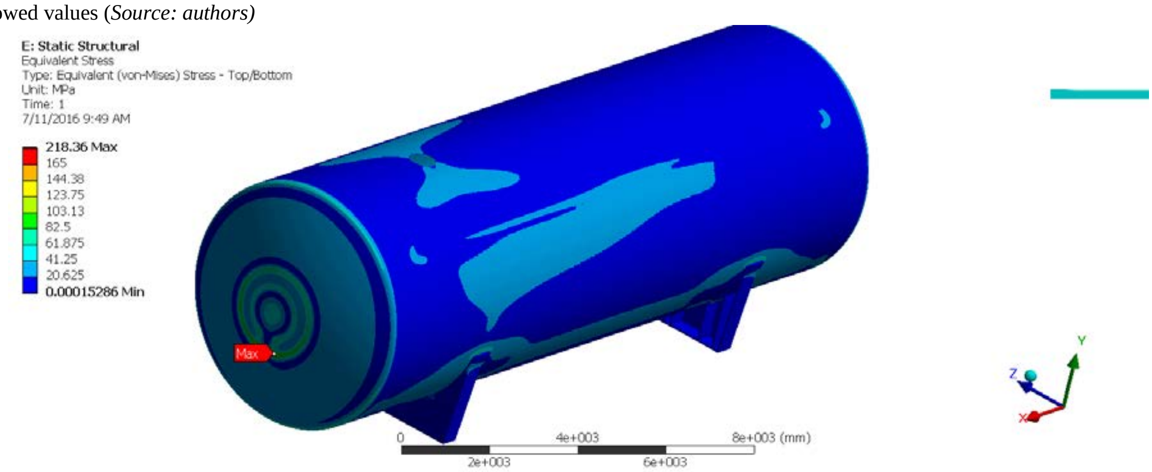

Figure 8 Load case 2 - stress distribution on outler shell *(Source: authors)*

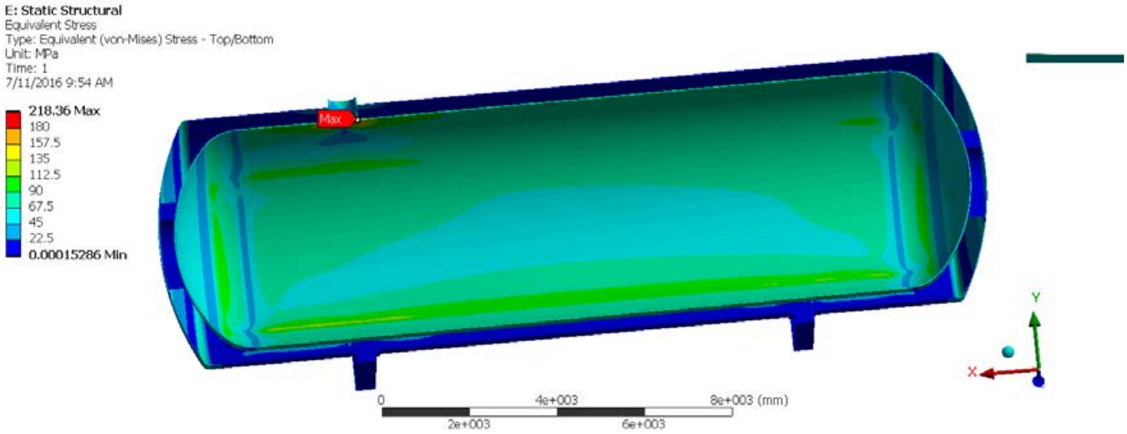

Figure 9 Load case 2 - Longitudinal crossection stress, distribution on inner shell *(Source: authors)*

Table 4 shows the maximum stress for inner and outer shell with a factor of safety that exceed the value of 1.7, which means that in this load state in terms of strength it produces some reserve.

Part	Equivalent von Misses stress [MPa]	Safety factor
Inner shell	218,36	1,74
Outer shell	119,06	1,72

Table 4 Load case 2, comparison of calculated values and allowed values (*Source: authors)*

5.4.3 Results for load state 3

In the third type of load the half symmetry of model was again used. Stress distribution can be observed on the outer and inner shell, the maximum stress occurred again in the front part of the outer shell (Figure 10) and in the area of filler neck in the inner shell (Figure 11).

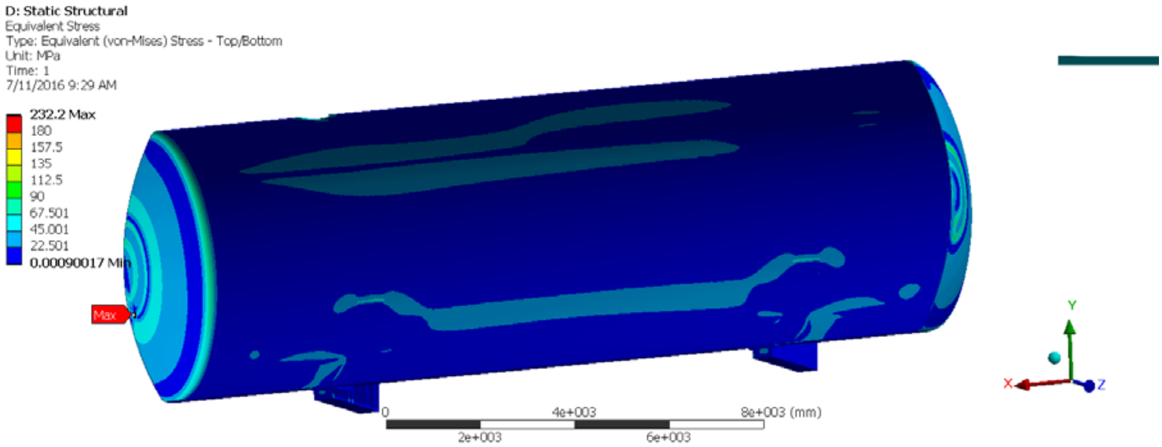

Figure 10 Load case 3 - stress distribution on outler shell *(Source: authors)*

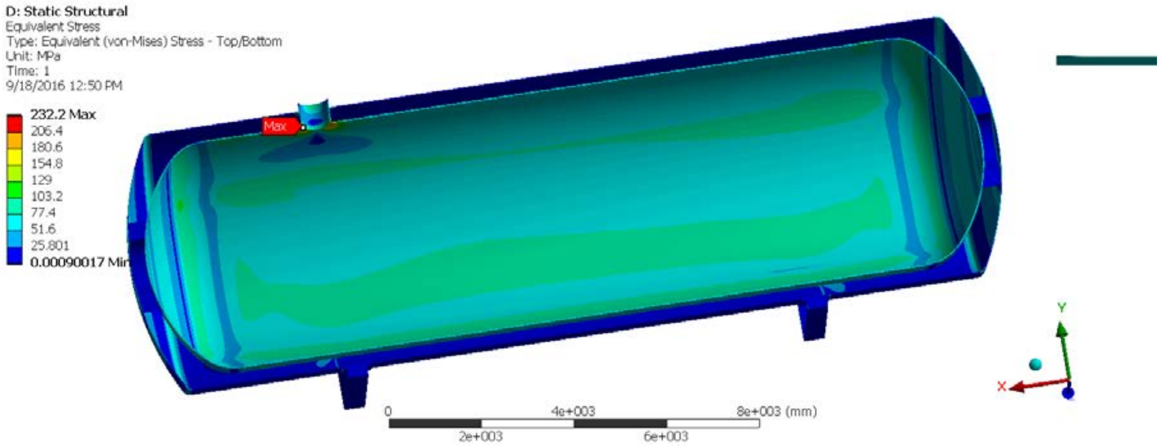

Figure 11 Load case 3 - Longitudinal crossection stress, distribution on inner shell *(Source: authors)*

Safety factor has exceeded the limit of 1.5 for this load case (Table 5). However, in dealing with the outer shell it exceeded the value of 2.

Part	Equivalent von Misses stress [MPa]	Safety factor
Inner shell	232,2	1,64
Outer shell	98,43	2,08

Table 5 Load case 3, comparison of calculated values and allowed values (*Source: authors)*

5.4.4 Results for load state 4

The stress distribution and the position of maximum stress can be seen in Figure 12) for the outer shell of tank and on the Figure 13) for inner shell of tank. For computation half symmetry was used.

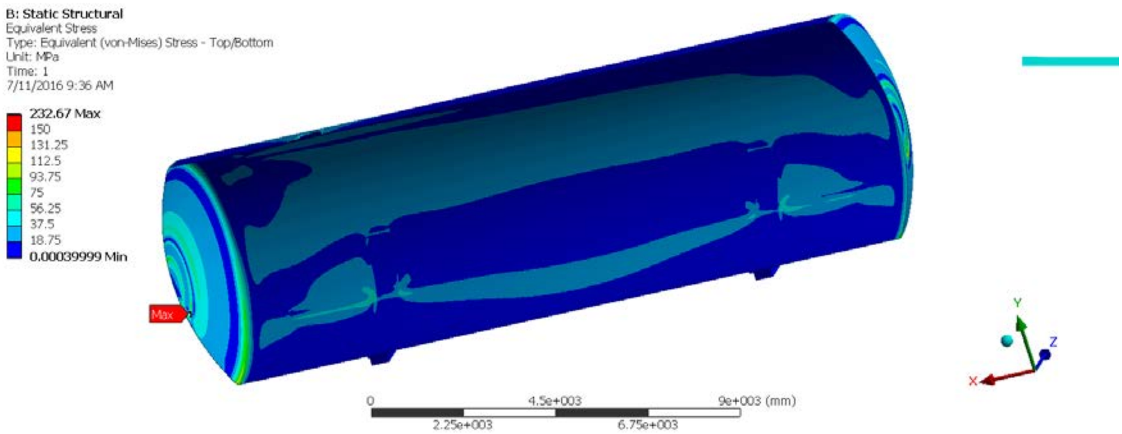

Figure 12 Load case 4 - stress distribution on outler shell *(Source: authors)*

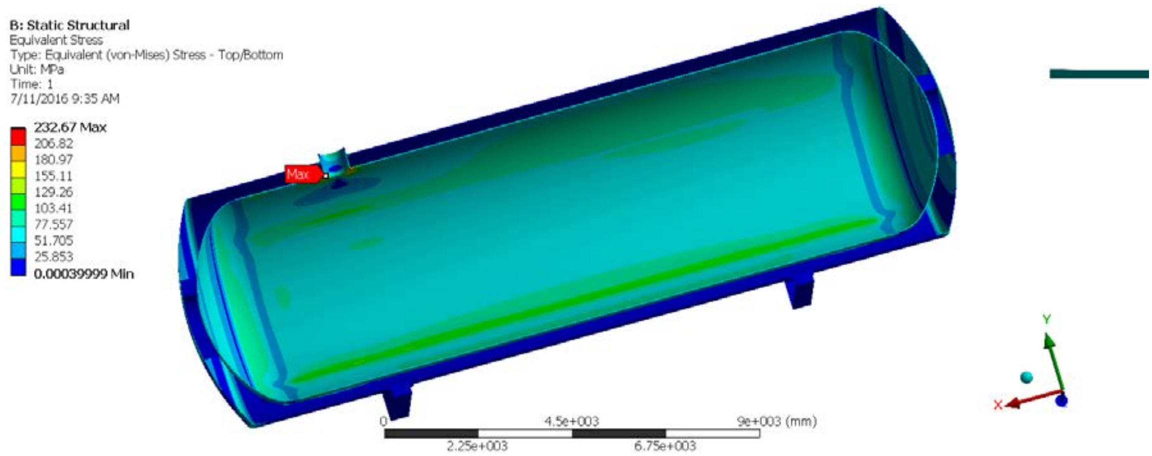

Figure 13 Load case 4 - Longitudinal crossection stress, distribution on inner shell *(Source: authors)*

The obtained values of the maximum stress and the calculated safety factor are given in Table 6. Coefficient of safety once again does not fall below the permissible value of 1.5, thus solved state can be considered suitable.

Part	Equivalent von Misses stress [MPa]	Safety factor
Inner shell	232,67	1,63
Outer shell	131,4	1,56

Table 6 Load case 4, comparison of calculated values and allowed values (*Source: authors)*

6 Conclusion

In all four load states areas with maximum stress were created in identical locations, in the case of outer shell as in the case of inner shell. In the outer shell, it was on the front face; the stress concentrator could be removed using a different type of knob block. Inner shell has stress concentrator always occur in the area of the filler neck. With given dimensions of the LNG tanks is in the construction this area the most loaded part and it is considered as the most critical point. In the future, it would be appropriate to optimize the area of filler neck, which means improved strength conditions while maintaining the smallest possible thermal transmittance. According to IMO: For each load, for portable tanks, the safety coefficient for metals having a clearly defined yield point should be 1.5 in relation to the determined yield stress. Every case of load suits to standard in computation of this volume (Table 3-6).

Literature:

1. Barta, D., Mruzek, M., Kendra, M., Kordos, P., Krzywonos, L.: *Using of non-conventional fuels in hybrid vehicle drives.* In: Advances in Science and Technology Research Journal, Lublin University of Technology, Volume 10, Issue 32, 2016. pp. 240 – 247. ISSN 2299-8624.

2. Buil, R.M., Hernando D.V. *Comparison of Heat Insulations for Cryogenic Tankers Using Analytical and Numerical Analysis.* Hindawi Publishing Corporation Advances in Mechanical Engineering, 2013. 17 p.

3. European Commission – *SEVESO III*. Available on: http://ec.europa.eu/environment

4. European Committee for Standardization (CEN). Available on: http://www.cen.eu/Pages/default.aspx

5. GIIGNL. *Basic Properties of LNG*. [online]. France. 9 p. Available on: http://www.giignl.org.

6. GIIGNL. *Managing LNG Risks*. [online]. France. 8 p. Available on: http://www.giignl.org.

7. Hoffman, A.: *The Thermal Conductivity of Cryogenic Insulation Materials and Its Temperature Dependence.* Cryogenics. 46, 2006. 815-824.

8. *IMO Guidance on the continued use of existing IMO type portable tanks and road tank vehicles for the transport of dangerous goods.* Ref.: T3/1.01 DSC/Circ.12 11 November 2003.

9. Lisowski, E., Czylycki, W., Lazarczyk, K.: *Using of polyamide in construction of supporting blocks of cryogenic tanks on example of LNG container.* Archives of Foundry engineering, Vol. 10, Is. 3, 2010. pp. 81-86.

10. Sebor, G., Pospisil, M., Zakovec, J.: *Technical and economic analysis of suitable alternative fuels for transport.* University of Chemistry and Technology, Prague. 2006.

11. Skrucany, T., Kendra, M., Sarkan, B., Gnap, J.: *Software simulation of an energy consumption and GHG production in transport.* In: Tools of transport telematics: 15th international conference on Transport systems telematics, TST 2015: revised selected papers: Wrocław, Poland, April 15-17, 2015. - Cham: Springer, 2015. pp. 151-160. ISBN 978-3-319-24576-8.

12. Stopka, O., Kampf, R.: *Determining the most suitable layout of space for the loading units' handling in the maritime port.* Transport, 12 April 2016. pp. 1-11. ISSN 1648-4142. DOI: 10.3846/16484142.2016.1174882.

13. Tropp, M., Handrik, M., Kopas, P., Saga, M.: *Computer simulation of induction bending process*. Pipeline and Gas Journal (239) 11, 2012.

Primary Paper Section: J

Secondary Paper Section: JR